

Effect of Framework Shape on the Fracture Strength of Implant-Supported All-Ceramic Fixed Partial Dentures in the Molar Region

Mitsuyoshi Tsumita, DDS, PhD,¹ Yuji Kokubo, DDS, PhD,¹ Per Vult von Steyern, LDS, PhD,² & Shunji Fukushima, DDS, PhD¹

¹ Department of Fixed Prosthodontics, Tsurumi University School of Dental Medicine, Tsurumi, Tsurumi-Ku, Yokohama, Japan

² Department of Prosthetic Dentistry, Malmö University Faculty of Odontology, Malmö, Sweden

Keywords

All-ceramic bridge; framework; FEM; fracture strength; dental implant.

Correspondence

Mitsuyoshi Tsumita, Tsurumi University School of Dental Medicine, Department of Fixed Prosthodontics, 2-1-3 Tsurumi, Tsurumi-Ku, Yokohama, Japan 230-8501.
E-mail: tsumita-mitsuyoshi@tsurumi-u.ac.jp

Accepted December 6, 2006.

doi: 10.1111/j.1532-849X.2007.00287.x

Abstract

Purpose: The aim of the present study was to clarify the effects of the shape of the zirconium framework of implant-supported, all-ceramic fixed partial dentures (FPDs) on the fracture strength and fracture mode.

Materials and Methods: This study consisted of mechanical strength testing and 3D finite element analysis (FEA). The three framework shapes used in this study were: (1) conventional shape (control); (2) convex shape: 1.0-mm curve in the direction of the occlusal surface; and (3) concave shape: 1.0-mm curve in the direction of the gingival surface. Five frameworks were made for each condition (total: 15). A load (N) was applied until the FPD fractured. For FEA, a 3D model consisting of cortical bone, cancellous bone, implant bodies, and superstructure was constructed.

Results: The results of the mechanical strength test showed that fracture load was 916.0 ± 150.1 N for the conventional shape, 1690.5 ± 205.3 N for the convex shape, and 1515.5 ± 137.0 N for the concave shape. The mean final fracture load for the FPDs with frameworks was the highest for the convex shape; however, a critical crack in the veneer porcelain (736.5 ± 145.2 N) was confirmed during loading for the convex shape. Stress distribution maps for all conditions showed that tensile stress was generated at the veneer porcelain on the gingival side of the mesial and distal connectors of the pontic; however, there were differences in the maximum value and stress distribution within the framework.

Conclusion: The shape of the framework, particularly the shape of the pontic–connector interface, affects the stress distribution, fracture strength, and fracture mode of all-ceramic FPDs, and stress concentration inside a framework may induce cracking of layering porcelain.

Due to superior esthetics and biocompatibility, all-ceramic crowns have become more popular in clinical practice, and many studies have demonstrated very favorable results.^{1–5} At the same time, some studies have been conducted to evaluate the clinical use of all-ceramic fixed partial dentures (FPDs);^{6–9} however, fractures of FPDs, in particular those originating on the gingival side of the connector, have been reported. In general, the use of many all-ceramic FPD systems is limited to the anterior region and is not recommended for the molar region.

According to a study by Sorensen et al,⁶ fractures were found in 7 out of 61 In-Ceram Alumina FPDs placed in the oral cavity (21 FPDs in the anterior region, 19 in the premolar region, and 21 in the molar region) before the 3-year recall. Of these seven FPDs, five were placed in the molar region and two in the

premolar region; however, none of the anterior FPDs fractured. In other words, 24% of the FPDs placed in the molar region fractured over a 3-year period, indicating that caution must be exercised when placing all-ceramic FPDs in this area.

On the other hand, Vult von Steyern et al⁷ clinically assessed 20 In-Ceram Alumina FPDs placed in the molar region over a 5-year period and reported that only two FPDs (10%) fractured. Olsson et al⁸ also documented that the 5- and 10-year cumulative survival rates for 42 In-Ceram Alumina FPDs (26 FPDs in the molar region, including cantilevers) were favorable (93% and 83%, respectively).

While there are several types of all-ceramic FPD systems, most systems consist of a high-strength core material and highly esthetic veneer porcelain. With the increased use of CAD/CAM

in dentistry, there has been a shift in the type of core material used from aluminum oxide (Al_2O_3) to zirconium oxide (ZrO_2); however, not many long-term clinical studies evaluating systems with ZrO_2 frameworks have been performed. Suarez *et al*⁹ conducted a 3-year clinical evaluation of the In-Ceram Zirconia system, the main component of which is Al_2O_3 , and reported no fractures in 18 posterior FPDs during the observation period.

To date, there is not sufficient clinical evidence for clinicians to justify placing all-ceramic FPDs in the molar region. We hypothesized that the shape of the all-ceramic FPD frameworks affects the fracture strength. Hence, the objective of the present study was to clarify the effect of the zirconium framework shape of implant-supported all-ceramic FPDs on the fracture strength and mode.

Materials and methods

This study consisted of mechanical strength testing and 3D finite element analysis (FEA).

Mechanical strength test

Prior to the preparation of the all-ceramic FPDs for the mechanical strength test, a substructure consisting of abutments, implants, and an acrylic block was prepared according to the method reported by Vult von Steyern *et al*.¹⁰

Abutments (Procera Abutment CAD, Nobel Biocare, Goteborg, Sweden) were attached to implants (Brånemark Mk III, $.4 \times 10$ mm, Nobel Biocare) using abutment screws and were fixed horizontally in holes prepared in an acrylic block (78-mm wide, 8-mm deep, 19-mm high) using New Fujirock (GC, Tokyo, Japan) die stone plaster. The distance between the implants from center to center was 17 mm.

Based on the completed substructure, a superstructure was made using the Cercon system (DeguDent, Hanau, Germany), which is a CAM-aided, all-ceramic system. The three framework shapes made of Cercon base used in this study were as follows: (1) conventional shape (control); (2) convex shape: 1.0-mm curve in the direction of the occlusal surface; and (3) concave shape: 1.0-mm curve in the direction of the gingival surface (Fig 1). Five frameworks were made for each condition (total: 15). Layering porcelain (Cercon Ceram S, DeguDent) was applied to the frameworks to be used as specimens for mechanical strength testing. The mesiodistal dimension of the completed FPD was 26 mm and of the pontic was 8 mm; the diameter of the framework connector was 3 mm. A completed

FPD was carefully fixed to the substructure. According to Filser *et al*'s method,¹¹ the FPD was not cemented.

The specimens were mounted in the testing jig of a mechanical testing machine (Auto Graph AGS-5kND, Shimadzu, Kyoto, Japan). A loading rod with a 2.0-mm radius tip was positioned in the center of the occlusal surface of the pontic, and a load (N) was applied at a crosshead speed of 0.5 mm/min until fracture (Fig 2). The load and time elapsed until specimen failure were recorded.

The fracture load was the maximum load in the resulting load-time curve diagram. Also, the initial crack load was the first significant load confirmed during flexure on the curve diagram before reaching the maximum load. The mean fracture load and initial crack load were calculated (SPSS 10.0.7J, SPSS, Chicago, IL). One-way ANOVA was applied to statistically determine significant differences. The significance level was established at a *p*-value < 0.05 . Differences between groups were identified with Tukey's test.

After the mechanical strength testing, scanning electron microscopic (SEM) analysis (JSM-T300, JEOL, Tokyo, Japan) was conducted on the surfaces of the fractured conventionally-shaped specimens. Specimens were gold sputter-coated (Quick Auto Coater SC-701AT, Sanyu Denshi, Tokyo, Japan) prior to SEM analysis.

Finite element analysis

Two types of models for analysis were prepared: fully assembled models including supporting tissue (cortical bone, cancellous bone, and implant bodies), and localized models that did not include the supporting tissue; in this case, the model was limited to the cervical area of the abutment neck.

Analyzing models

An implant-supported, 3-unit FPD was designed to be placed in the first premolar and first molar region of a patient with missing lower left molars, and a 3D model consisting of cortical bone, cancellous bone, implant bodies, and implant prostheses was constructed (Fig 3). Brånemark Mk III $.4 \times 10$ mm implant bodies were used with Cercon system prostheses. The mesiodistal dimension of the FPD was 26 mm, the intercenter distance of the implants was 17 mm, the mesiodistal dimension of the pontic was 8 mm, and the diameter of the framework connector was 3 mm. These parameters were the same as for the mechanical strength test.

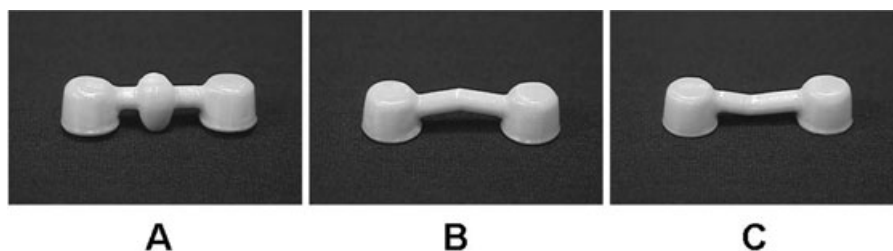


Figure 1 Shape of framework: (A) conventional shape; (B) convex shape (1.0-mm curve in the direction of the occlusal surface); (C) concave shape (1.0-mm curve in the direction of the gingival surface).

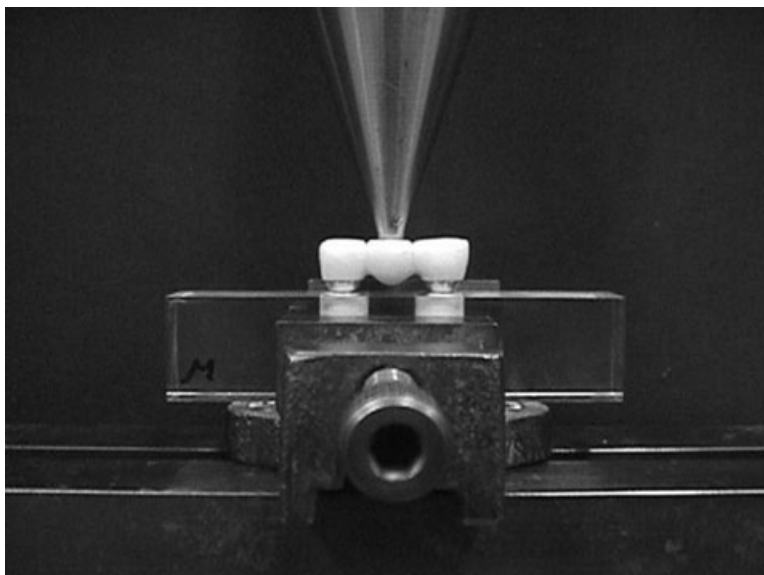


Figure 2 Mechanical strength test. A loading rod was positioned in the center of the occlusal surface of the all-ceramic pontic and loaded until fracture occurred.

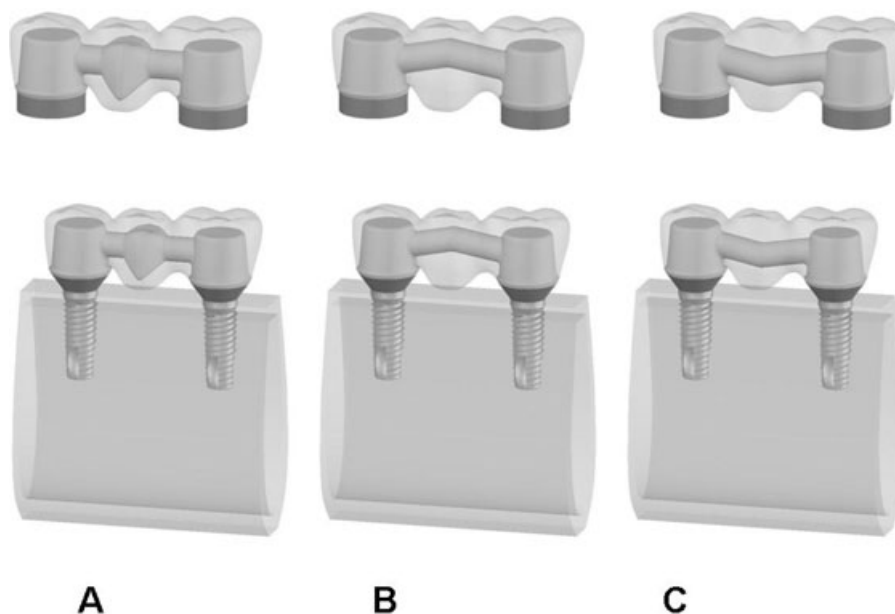


Figure 3 Analysis models. The analysis models without support tissues (upper view), and models with support tissues (lower view): (A) conventional shape; (B) convex shape (1.0-mm curves in the direction of the occlusal surface); (C) concave shape (1.0-mm curves in the direction of the gingival surface).

To prepare the analysis models, all-ceramic FPDs were fabricated at the laboratory, and each FPD was scanned by micro computed tomography (CT) (MCT-100MF, Hitachi Medical, Tokyo, Japan). The micro CT data were converted to Digital Imaging and Communications in Medicine (DICOM) data. To prepare a 3D image, 202 DICOM scans were subjected to segmentation (ZedView, LEXI, Tokyo, Japan) to generate standard template library (STL) data. Furthermore, using RapidForm (INUS Technology, Seoul, Korea), non-uniform rational B splines (NURBS) surfaces were prepared and converted to initial graphics exchange specification (IGES)

data. SolidWorks 2005 (3D CAD, SolidWorks, Concord, MA) was used for IGES data processing and analysis model preparation.

Material properties

The Young's modulus (E) and Poisson's ratio (ν) of the FPD frameworks (Cercon smart ceramics) and veneer porcelain (Cercon Ceram S) were based on the manufacturer's values, and those for cortical bone, cancellous bone, and implant body were based on a past report¹² (Table 1).

Table 1 Material properties

Material	Elastic modulus (MPa)	Poisson's ratio
Cercon framework	21,000*	0.23
Cercon Ceram S	70,000*	0.23
Titanium (implant and abutment)	110,000†	0.35
Cortical bone	13,700†	0.3
Cancellous bone	1370†	0.3

*DeguDent Gesellschaft mit beschränkter Haftung, Germany (information provided by the manufacturer).

†Eskitacioglu et al. The influence of occlusal loading location on stresses transferred to implant-supported prostheses and supporting bone. A three-dimensional finite element study. *J Prosthet Dent* 2004; 91: 144–150.

Boundary and loading conditions

At the center of the pontic, a load-bearing zone with a 2-mm radius was established, and an 800 N load¹³ (assumed maximum occlusal force) was applied orthogonal to the occlusal plane.

For the models that included the supporting tissue, the restricted points were all nodes of the mesial wall of bone, of the distal wall of bone, and of the lower margin of cortical bone. For the models without the supporting tissue, the restricted points were the inferior surfaces of the mesial and distal abutments.

Test conditions of framework

As was the case with the mechanical strength testing, the following three framework shapes were established: (1) conventional shape (control), (2) convex shape: 1.0-mm curve in the direction of the occlusal surface, and (3) concave shape: 1.0-mm curve in the direction of the gingival surface.

Mesh generation and data processing

Mesh generation and data processing were carried out using COSMOS Works 2005 (SolidWorks). The mesh consisted of 3D tetrahedral solid elements with an element size of 1 mm and an allowable error of 0.05 mm. For the models including the supporting tissue, the conventional type had 142,121 nodes and 100,808 elements; the convex type had 144,112 nodes and 102,315 elements; and the concave type had 144,052 nodes and 102,289 elements. For the models without the supporting tissue, the conventional type had 22,592 nodes and 15,046 elements; the convex type had 24,338 nodes and 16,358 elements; and the concave type had 23,701 nodes and 15,891 elements (Fig 4).

Results

Mechanical strength test

The results of mechanical strength testing for the implant-supported, all-ceramic FPDs with a zirconium framework showed that the fracture load was 916.0 ± 150.1 N for the conventional shape, 1690.5 ± 205.3 N for the convex shape, and 1515.5 ± 137.0 N for the concave shape. A significant difference existed between the conventional shape and the other two shapes ($p < 0.05$). The mean initial crack load for the conventional shape was 681.5 ± 267.0 N, 439.0 ± 113.4 N for the convex shape, and 945.0 ± 380.7 N for the concave shape (Fig 5).

The mean final fracture load for the FPDs with frameworks was the highest for the convex shape, although a critical crack in the veneer porcelain (736.5 ± 145.2 N) was confirmed during loading for all these specimens (Fig 6). The cracks originated in the lower margin of the pontic framework and grew towards the gingival surface of the medial and distal connectors of the pontic.

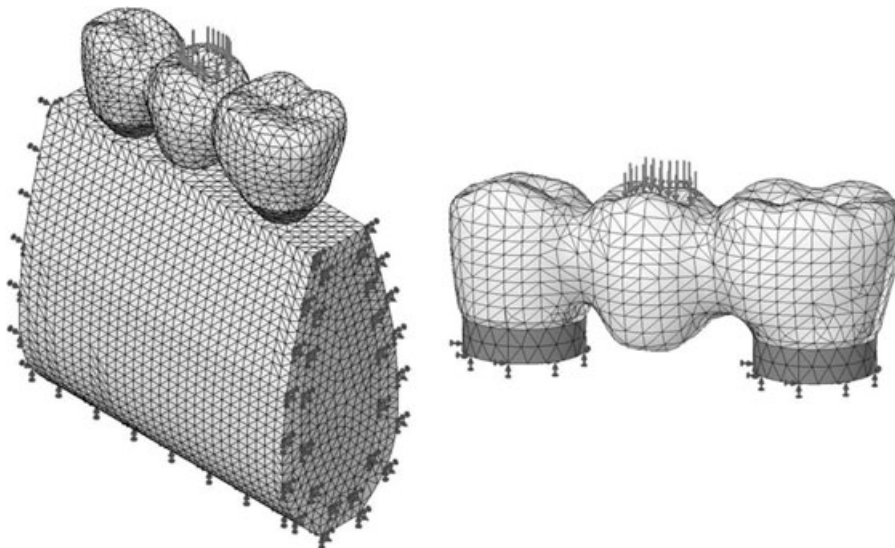


Figure 4 Mesh generation. The analysis model with support tissues (left), and model without support tissues (right). A simulated load of 800 N was applied at the center of the pontic. In the left model, the boundary condition with no displacement was prescribed at the mesial cross-section, distal cross-section, and lower surface of mandible and fixed at the cut plane of the abutments in the right model.

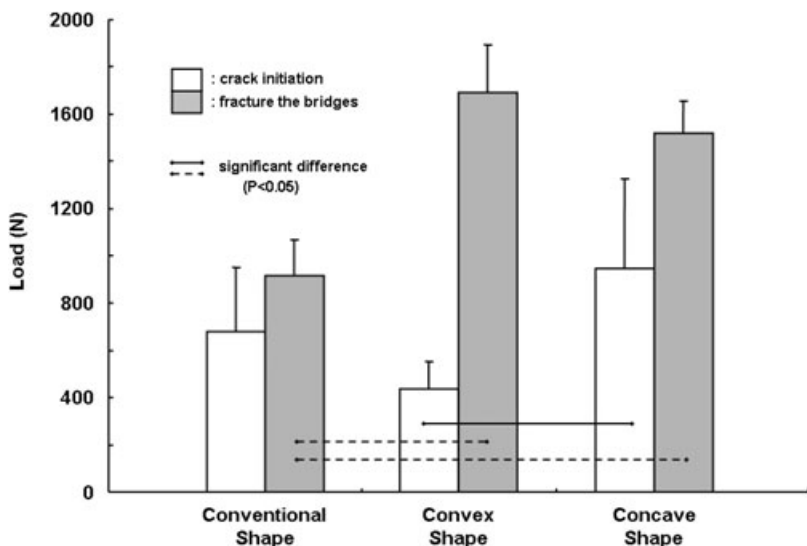


Figure 5 Results of the mechanical strength test [load that initiated cracking in the veneer porcelain (white bars), and the load required to fracture the bridges (gray bars)].

SEM analysis

The fracture in the conventional shape originated in the gingival side of the distal connector, as reported by Sorensen *et al.*⁶ Figures 7 and 8 show the SEM images of the fractured surface of the conventional shape following mechanical strength testing. The interface between the framework and layering porcelain had exfoliated in most parts. Also, air bubbles of various sizes were located in the layering porcelain.

Finite element analysis

In the past, several studies on ceramic restorations using FEA used the von Mises stress;^{12,14-16} however, tensile stress is important for fragile materials, and in the present study, the maximum principal stress was also investigated in addition to the von Mises stress. Stress distribution maps for all conditions

showed that the tensile stress was generated at the veneer porcelain on the gingival side of the mesial and distal connectors of the pontic; however, there were differences in the maximum value and stress distribution within the framework (Figs 9, 10). On the gradation bar for maximum principal stress distribution, negative values indicate compressive stress, while positive values indicate tensile stress. The combined results of the analysis for all components of each model are represented in Figures 11-13.

Localized model

For the models limited to the cervical area of the abutments, the von Mises stress was the greatest inside the framework of the mesial margin of the distal abutment for the conventional, convex, and concave shapes (85.7, 85.8, and 87.6 MPa,

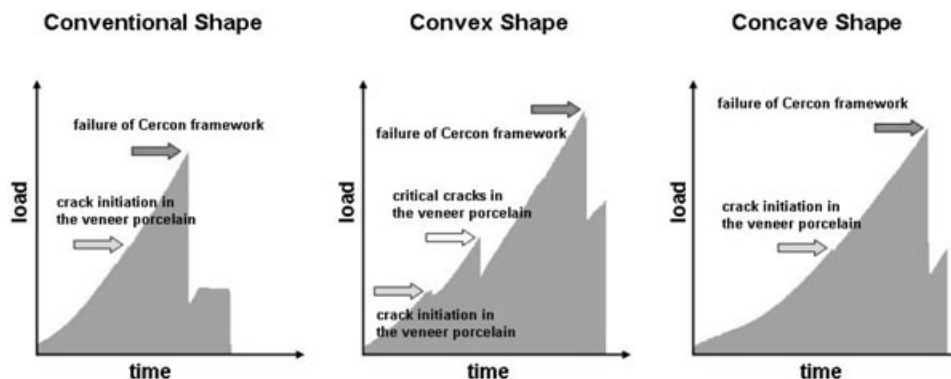


Figure 6 Load-time curve diagrams. Typical load-time diagrams and failure behavior of each condition. Left: bridge with conventional shape framework showed a failure of the framework and the veneer at the same time. Center: bridge with convex shape framework showed critical cracks in the veneer porcelain before the failure of framework. Right: bridge with concave shape framework showed a failure of the framework and the veneer at the same time.

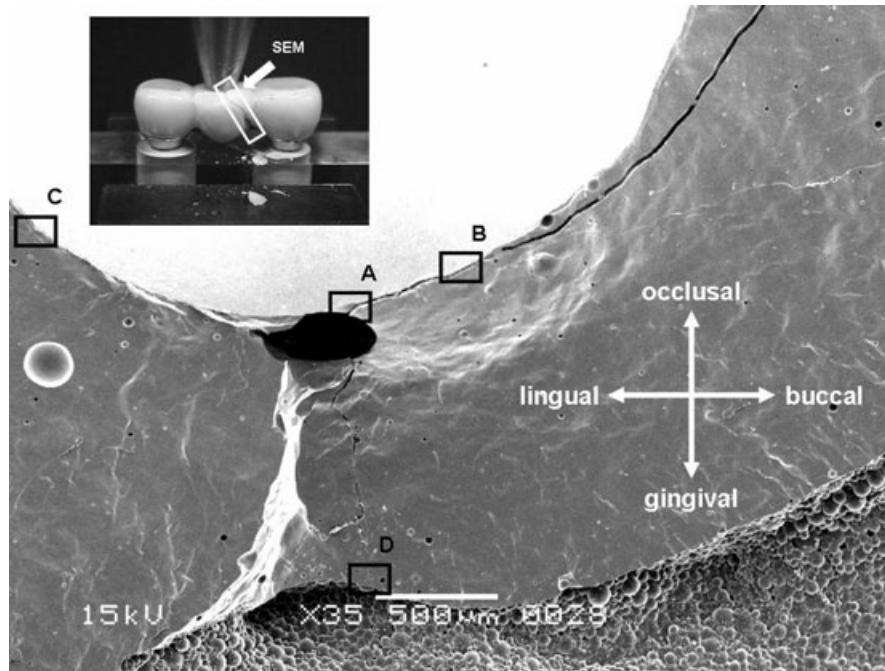


Figure 7 Fracture surface of Cercon FPD with conventionally shaped framework. The rectangle areas (A–D) indicate the magnification points in Figure 8.

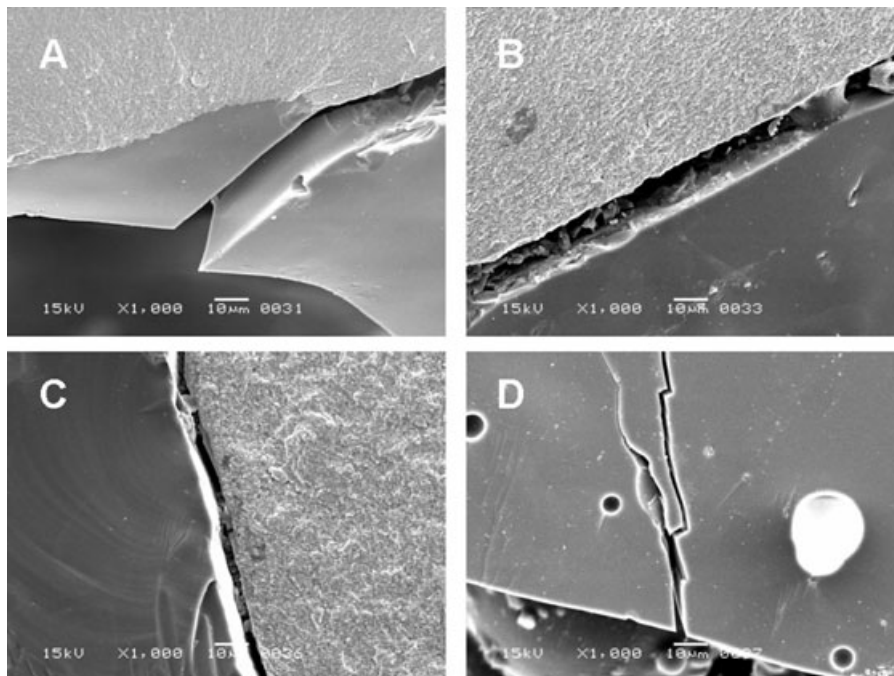


Figure 8 (A–C) Exfoliation of the porcelain–framework interface at gingival side (A), buccal side (B), and lingual side (C). (D) Air bubbles of various sizes were located in the outermost layer of porcelain, and the crack extended to this area.

respectively). The maximum principal stress distribution for the conventional, convex, and concave shapes was the greatest at the veneer porcelain on the gingival side of the distal connector (32.0, 33.3, and 32.1 MPa, respectively).

Full assembly model

For the fully assembled models including the supporting tissue, the von Mises stress was the greatest at the mesial cervical

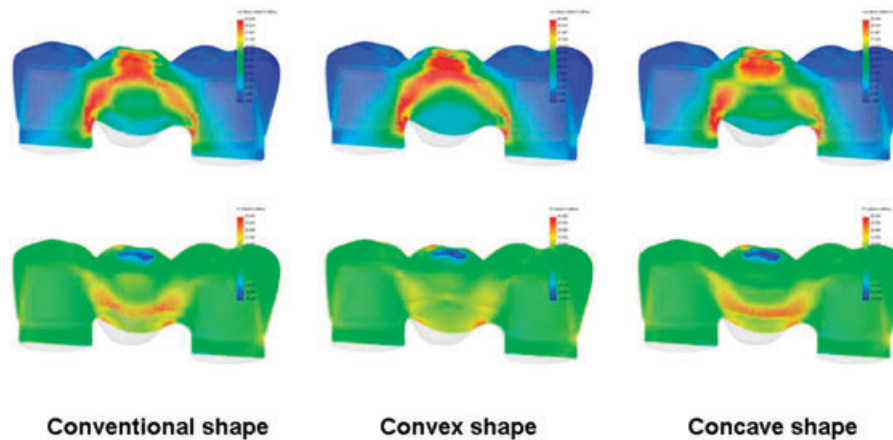


Figure 9 Stress distributions on the localized models. Distributions of Von Mises stress (upper view), and maximum principal stress (lower view) at mesiodistal cross-section.

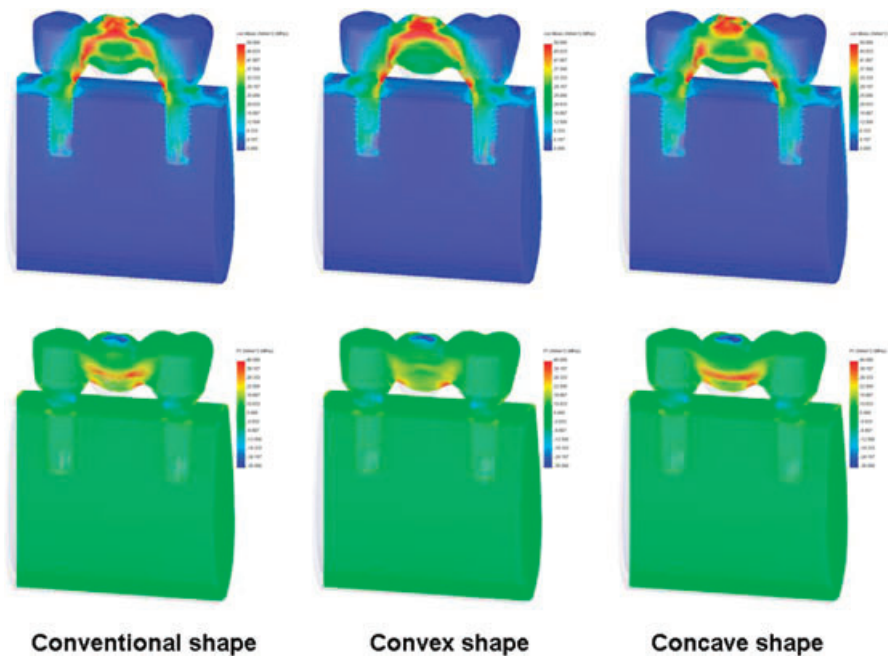


Figure 10 Stress distributions on the fully assembled models. Distributions of von Mises stress (upper view) and maximum principal stress (lower view) at mesiodistal cross-section.

area of the distal abutment for the conventional model (73.1 MPa), at the distal cervical area of the mesial abutment for the convex model (70.2 MPa), and within the veneer porcelain for the concave model (75.2 MPa). In terms of the maximum principal stress distribution, the stress was the greatest at the veneer porcelain on the gingival side of the distal connector for the conventional, convex, and concave shapes (47.7, 49.3, and 46.5 MPa, respectively).

The von Mises stress was high for the implants at the defect-side abutment connector. Compared to the implants placed on the distal side, the von Mises stress was higher for the implants placed on the mesial side. Also, the maximum principal stress

was high at the first thread inferior surface. The maximum principal stress was higher for the implants placed on the mesial side compared to the distal side.

Discussion

In the past, it was believed that the fracture of all-ceramic FPDs was caused by insufficient mechanical strength or air bubble contamination.¹⁷ To increase the mechanical strength, the framework is now made of ZrO_2 instead of Al_2O_3 ; however, few long-term clinical studies on ZrO_2 frameworks have been conducted.

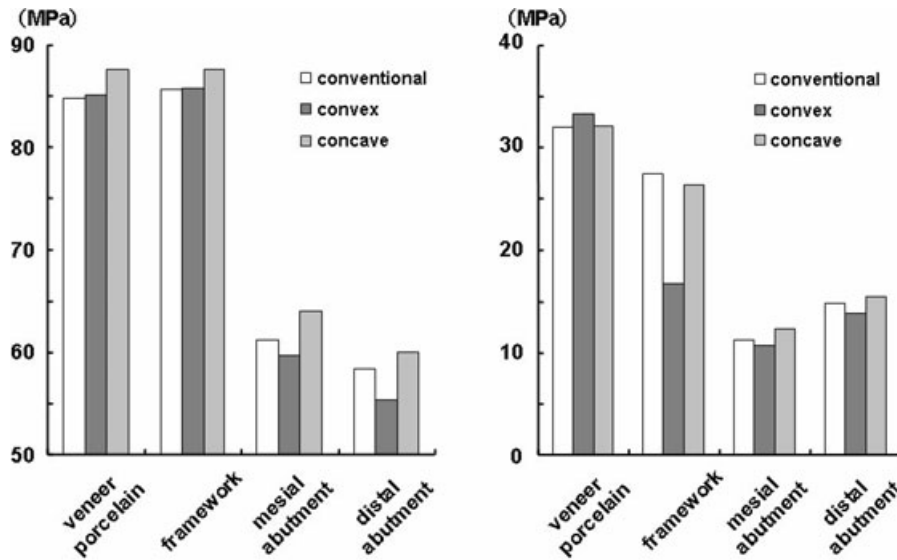


Figure 11 Results of FEA of the localized models. Two bar graphs showing the von Mises stress (left) and the maximum principal stress (right) in each component.

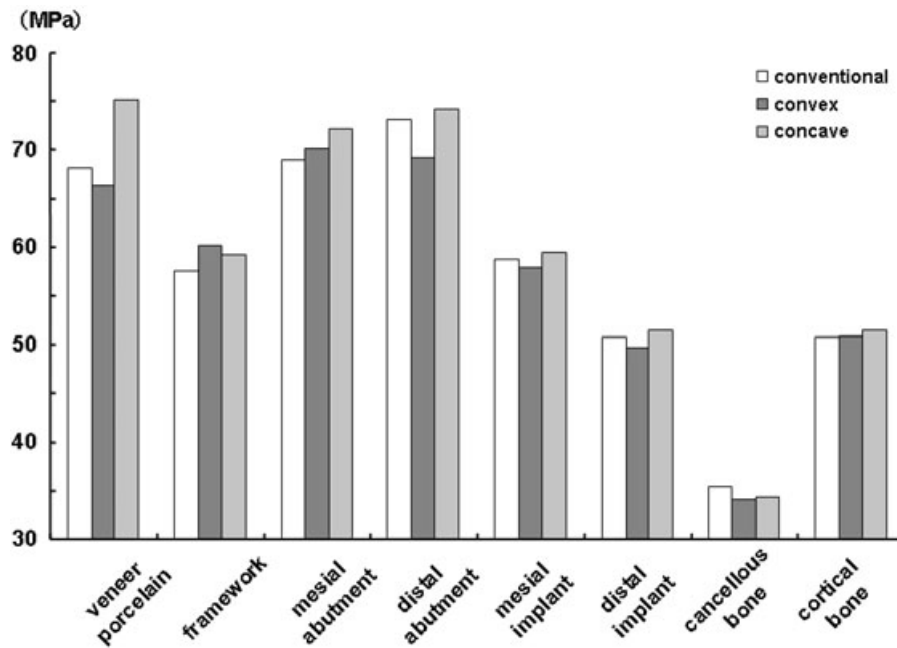


Figure 12 The von Mises stress generated in each component.

When fusing the porcelain to a metal FPD frame, the difference in firing shrinkage generates internal stress that causes cracks and fractures if the thickness of the porcelain is uneven. Therefore, the metal frame design is based entirely on the shape of the final prostheses. The framework shape of the all-ceramic FPDs generally used today follows this principle; however, differences in firing shrinkage are almost nonexistent with all-ceramic FPDs. Therefore, the pontic framework in the present study was made in three shapes, and a mechanical strength test

and stress analysis were carried out using frameworks made of ZrO₂.

The finite element method used for the present analysis has been employed and documented extensively in dentistry.^{12,14-16,18-23} Any shape can be easily analyzed with this method, and because the area of analysis itself is made into a model, it is possible to express property changes in it. This method is also widely used in areas such as statics, kinetics, collision, heat conduction, fluid, and electromagnetic fields.

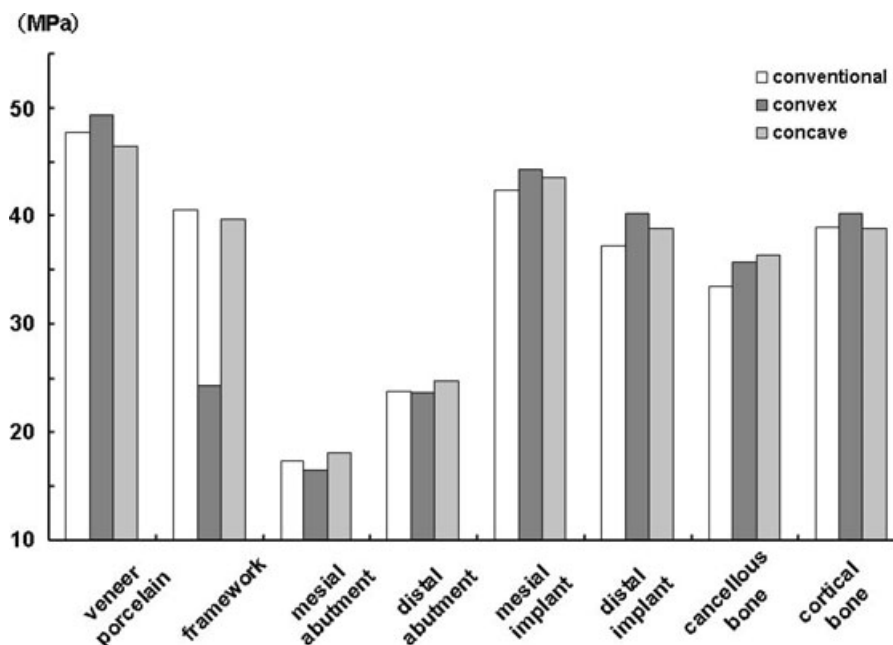


Figure 13 The maximum principal stress generated in each component.

Furthermore, it can simultaneously handle multiple fields, such as thermal stress.

Increasing the cross-sectional area of the connector is generally recommended to improve the fracture strength of the FPDs. This method has been clarified by some studies using the finite element method;^{14,20} however, there are clinical morphological and esthetic limitations to increasing the cross-sectional area of a connector. Hence, it is thought that the fracture strength of all-ceramic FPDs would depend on the strength of the material used to fabricate the framework; however, the results of the present study suggest the possibility that even when using the same material, an FPD can be made to withstand more stress through stress dispersion by altering the shape of the framework of the pontic. Oh *et al*²¹ analyzed the relationship between the stress distribution of FPDs and the curvature radius of the connector upper and lower embrasures using the 3D finite element method. They reported that the curvature radius of the lower embrasure strongly affected the fracture resistance of all-ceramic FPDs; however, because their analysis model was a single-mass FPD without a framework, further investigation is necessary for all-ceramic FPDs with a framework. In the present study, the connector of the lower embrasure was made into a U-shape as much as possible, as reported by Vult von Steyern *et al*.¹⁰

In this study, the diameter of the connector of framework was designed to be 3 mm. Filser *et al*¹¹ designed the cross-sectional area of the connector of framework to be 6.9 mm² (2.7×2.6); however, Raigrodski²⁴ states that the minimum critical connector surface area is 9 mm². Furthermore, Vult von Steyern *et al*⁷ designed the superoinferior height of the connector of framework to be 3 mm based on studies by Futterknecht and Jinoian²⁵ and obtained favorable results. Hence, the cross-sectional area for the present study appears to be valid.

Shape of frameworks within all-ceramic FPDs

The load applied to the center of the pontic reached the upper margin of the framework via the veneer porcelain and was dispersed in various ways, depending on the framework shape. The results of mechanical strength testing showed that the fracture load for the convex and concave shapes was significantly higher than for the conventional shape. The fracture load for the conventional shape was low, because there was an area of stress concentration inside the framework, which could be deduced by comparing the fracture mode of FPDs determined by the mechanical strength test and the maximum principal stress distribution results from the FEA (Fig 14). In other words, the mechanical strength test showed that the line connecting the veneer porcelain on the gingival side of the distal connector (where the principal stress distribution was the greatest), the pontic-connector interface (where stress concentrated in the framework), and the loading area demonstrated a typical failure mode for the conventional shape. It follows from this finding that the stress concentration inside a framework may induce cracking of the veneer porcelain. Similar findings were also obtained for the convex and concave shapes. This inference shows that the analysis model used in this research is very useful for predicting the fracture mode. Sorensen *et al*⁶ reported that all-ceramic molar FPDs usually fractured clinically at the distal connector. The results of the mechanical strength test in the present study also showed that the area of fracture was the same in the conventional shape, suggesting that there was no marked difference in the failure mode between the all-ceramic bridges with Al₂O₃ frameworks and those with ZrO₂ frameworks. Furthermore, it was clarified that the mode of fracture varied with the shape of the framework, even if the frameworks were made of the same material.

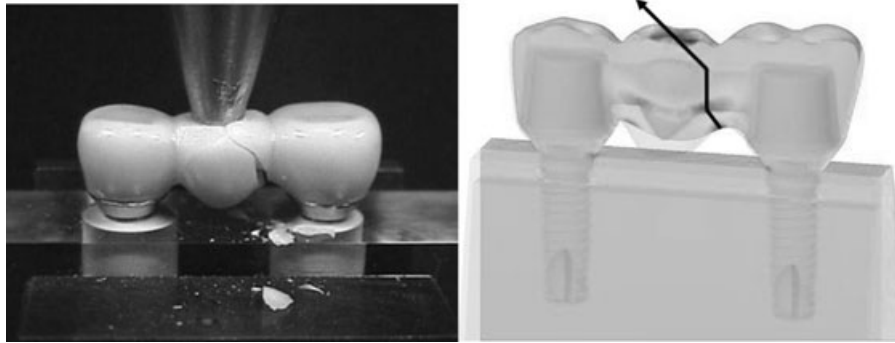


Figure 14 Failure mode. Left: typical failure mode of Cercon bridges with conventionally shaped framework. The fracture started from the gingival side of the connector, and the fracture surface propagated to the loading point. Right: schematic illustration of crack formation (black arrow).

The results of the mechanical strength test showed that the fracture load for the convex shape was the highest; however, critical cracks in the veneer porcelain were seen in the convex shape, but not in the other two shapes. These cracks occurred from the lower margin of the pontic framework towards the gingival surface of the medial and distal connectors of the pontic. Such failure is not clinically acceptable. Because of the geometry of the convex shape, it was difficult for the frameworks located on the gingival side of the connector where stress concentrates; thus, the veneer porcelain received the tensile stress directly, and cracks were initiated at a low load value. Also, the final fracture load was high, because the shape of frameworks resembled a reverse-catenary, and thus received the loading stress as compressive stress.

The fracture load for the concave shape was significantly higher than that for the conventional shape; the veneer porcelain cracking load for the concave shape was significantly greater than that for the convex shape. In terms of bridge engineering, the concave shape resembled a catenary; however, by arranging a framework without a pontic–connector interface where stress concentrates in an area of maximum principal stress, the load could be evenly dispersed throughout the lower margin of the frame.

Layering porcelain–framework interface

Filser *et al*¹¹ analyzed all-ceramic FPDs with a zirconium framework and reported that fractures occurred at the framework and layering porcelain interface and extended along the interface. They also reported the existence of a “stop and go” mechanism, which is not found with Al_2O_3 frameworks. As shown by the load–time curve diagrams in this study (Fig 6), a “stop and go” mechanism was also observed. In addition, SEM analysis of the connectors following failure showed circumferential peeling at the veneer porcelain and framework interface, indicating that it will be necessary to investigate the adhesion between the veneer porcelain and framework.

As reported by Kokubo and Shimoda,¹⁷ SEM analysis confirmed the presence of air bubbles within the all-ceramic FPDs. All air bubbles were inside the layering porcelain, and none were seen in the framework. With the increasing use of

CAD/CAM, the incidence of air bubble contamination inside the framework has decreased; however, due to esthetic requirements, the veneer porcelain must be applied in the conventional manner, and some air bubble contamination may be unavoidable. It is necessary to find a way to minimize air bubble contamination in the veneer porcelain. Also, some studies¹¹ have found that the origin of cracks in all-ceramic FPDs with zirconium frameworks was at the layering porcelain and framework interface. In the present study, the origin could not be identified, although crack extension around the layering porcelain and framework interface was confirmed.

FEA models

In the past, studies reproduced the periodontal ligament for FEA of natural tooth-supported, 3-unit FPDs;^{14,18,22} however, the physical properties of the periodontal membrane were estimated and were not actual values.²² Therefore, implant-supported FPDs without a periodontal ligament were used in this study to eliminate uncertain elements and clarify the effects of the framework shape.

Teeth are 3D objects, and their movements are also 3D. When analyzing isolated anterior tooth crowns, there is no problem with using the 2D finite element method, because the movement elements are mostly limited to the labiolingual plane.¹⁵ However, movement elements vary when analyzing molar FPDs. Therefore, this study employed a 3D finite element method. When constructing 3D analysis models, it is very difficult to reproduce the morphology of the occlusal surface in three dimensions by CAD. Hence, data in the present study were obtained by micro CT. In general, segmentation of DICOM data yields STL data. STL data are polygon data; there are no curve data. Therefore, by forming NURBS surfaces using STL data, IGES data with curve data were generated to allow CAD processing. It was always possible with this method to construct more realistic analysis models with smoother occlusal surfaces.

Localized models without supporting tissue and fully assembled models with supporting tissue were prepared. Several previous studies employing the finite element method used analysis models without supporting tissue;^{15,16,19–21,23} however, the effects of these tissues on analysis results have not been investigated. The maximum principal stress is important for fragile

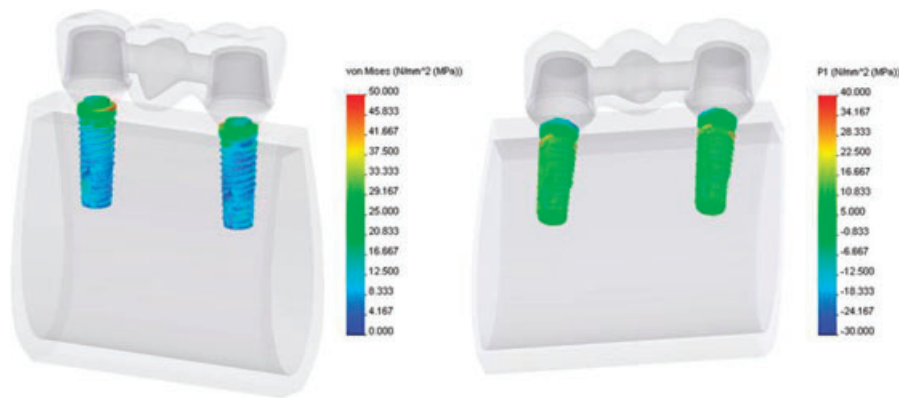


Figure 15 Stress distributions within implants—Von Mises stress (left), and maximum principal stress (right).

materials, and the results of the present study showed that the maximum principal stress for the localized models was as small as 15.4 MPa at the veneer porcelain, 11.3 MPa at the framework, 5.9 MPa at the mesial abutment, and 9.4 MPa at the distal abutment. These findings suggest that the maximum principal stress may be underestimated by analyses using localized models.

For all models, the maximum principal stress distribution was the greatest at the veneer porcelain of the distal connector, which is different from the results of our previous study on stress analysis of all-ceramic FPDs with an Al_2O_3 framework (In-Ceram Alumina).²⁶ The maximum principal stress with In-Ceram Alumina was the greatest within the framework on the gingival side of the distal connector. While this could be attributed to the difference in elastic modulus, it suggests the necessity for the optimization of frame shape for each material.

The von Mises stress for implants was high at the defect-side abutment connector, and the maximum principal stress was high at the first thread inferior surface. The von Mises stress and maximum principal stress of the mandible were high at the cortical bone. While stress was generated in cancellous bone, the level of stress was generally lower compared to cortical bone. This difference is due to the resorption of the cortical bone at the cervical area of implants *in vivo* (Fig 15).

A highly useful analysis was carried out in this study by gathering micro CT data and reproducing models with supporting tissue. Further investigations will be necessary to establish metal-free restorations by comparing them with natural-tooth models with the periodontal ligament.

Conclusion

To test the hypothesis that the shape of the framework of all-ceramic FPDs affects fracture strength, the shape of the framework of implant-supported, 3-unit, all-ceramic FPDs placed in the lower left first premolar and first molar region was analyzed by a mechanical strength test and 3D FEA. The following conclusions were obtained:

1. The shape of the framework, particularly the shape of the pontic–connector interface, affects the stress distribution, fracture strength, and fracture mode of all-ceramic FPDs.

2. Stress concentration inside a framework may induce cracking of the veneer porcelain.
3. Compared to analysis models with supporting tissue, FEA using models without supporting tissue may underestimate the maximum principal stress.

References

1. Odén A, Andersson M, Krystek-Ondracek I, et al: Five-year clinical evaluation of Procera AllCeram crowns. *J Prosthet Dent* 1998;80:450-456
2. McLaren EA, White SN: Survival of In-Ceram crowns in a private practice: a prospective clinical trial. *J Prosthet Dent* 2000;83:216-222
3. Segal BS: Retrospective assessment of 546 all-ceramic anterior and posterior crowns in a general practice. *J Prosthet Dent* 2001;85:544-550
4. Ödman P, Andersson B: Procera AllCeram crowns followed for 5 to 10.5 years: a prospective clinical study. *Int J Prosthodont* 2001;14:504-509
5. Gemalmaz D, Ergin S: Clinical evaluation of all-ceramic crowns. *J Prosthet Dent* 2002;87:189-196
6. Sorensen JA, Kang SK, Torres TJ, et al: In-Ceram fixed partial dentures: three-year clinical trial results. *J Calif Dent Assoc* 1998;26:207-214
7. Vult von Steyern P, Jonsson O, Nilner K: Five-year evaluation of posterior all-ceramic three-unit (In-Ceram) FPDs. *Int J Prosthodont* 2001;14:379-384
8. Olsson KG, Furst B, Andersson B, et al: A long-term retrospective and clinical follow-up study of In-Ceram Alumina FPDs. *Int J Prosthodont* 2003;16:150-156
9. Suárez MJ, Lozano JF, Paz Salido M, et al: Three-year clinical evaluation of In-Ceram Zirconia posterior FPDs. *Int J Prosthodont* 2004;17:35-38
10. Vult von Steyern P, al-Ansari A, White K, et al: Fracture strength of In-Ceram all-ceramic bridges in relation to cervical shape and try-in procedure. An *in-vitro* study. *Eur J Prosthodont Restor Dent* 2000;8:153-158
11. Filser F, Kocher P, Weibel F, et al: Reliability and strength of all-ceramic dental restorations fabricated by direct ceramic machining (DCM). *Int J Comput Dent* 2001;4:89-106
12. Eskitascioglu G, Usumez A, Sevimay M, et al: The influence of occlusal loading location on stresses transferred to implant-supported prostheses and supporting bone: a

- three-dimensional finite element study. *J Prosthet Dent* 2004;91:144-150
13. Kelly JR: Ceramics in restorative and prosthetic dentistry. *Annu Rev Mater Sci* 1997;27:443-468
 14. Kamposiora P, Papavasiliou G, Bayne SC, et al: Stress concentration in all-ceramic posterior fixed partial dentures. *Quintessence Int* 1996;27:701-706
 15. Magne P, Douglas WH: Design optimization and evolution of bonded ceramics for the anterior dentition: a finite-element analysis. *Quintessence Int* 1999;30:661-672
 16. Lang BR, Maló P, Guedes CM, et al: Procera AllCeram bridge. *Appl Osseointegration Res* 2004;4:13-21
 17. Kokubo Y, Shimoda S: Nondestructive examination of all-ceramic fixed partial denture with microcomputed tomography. *J Prosthet Dent* 2003;89:324
 18. Farah JW, Craig RG, Meroueh KA: Finite element analysis of three- and four-unit bridges. *J Oral Rehabil* 1989;16:603-611
 19. Kelly JR, Tesk JA, Sorensen JA: Failure of all-ceramic fixed partial dentures in vitro and in vivo: analysis and modeling. *J Dent Res* 1995;74:1253-1258
 20. Augereau D, Pierrisnard L, Barquins M: Relevance of the finite element method to optimize fixed partial denture design. Part I. Influence of the size of the connector on the magnitude of strain. *Clin Oral Investig* 1998;2:36-39
 21. Oh W, Gotzen N, Anusavice KJ: Influence of connector design on fracture probability of ceramic fixed-partial dentures. *J Dent Res* 2002;81:623-627
 22. Arai I, Tanaka Y, Shinki T: Analysis on occlusal force supporting mechanism of periodontium. *J Jpn Soc Stomatognath Funct* 2002;8:107-116
 23. Fischer H, Weber M, Marx R: Lifetime prediction of all-ceramic bridges by computational methods. *J Dent Res* 2003;82:238-242
 24. Raigrodski AJ: Clinical and laboratory considerations for the use of CAD/CAM Y-TZP-based restorations. *Pract Proced Aesthet Dent* 2003;15:469-476
 25. Futterknecht N, Jinoian V: Renaissance in der Vollkeramik. *Quintessenz Zahntech* 1990;16:1185-1197, 1323-1335
 26. Tsumita M, Kokubo Y, Ohtsuka T, et al: Influences of core frame design on the mechanical strength of posterior all-ceramic fixed partial dentures. Part 1. Two-dimensional finite element analysis. *Tsurumi Univ Dent J* 2005;31:203-210

Copyright of Journal of Prosthodontics is the property of Blackwell Publishing Limited and its content may not be copied or emailed to multiple sites or posted to a listserv without the copyright holder's express written permission. However, users may print, download, or email articles for individual use.

Copyright of Journal of Prosthodontics is the property of Blackwell Publishing Limited and its content may not be copied or emailed to multiple sites or posted to a listserv without the copyright holder's express written permission. However, users may print, download, or email articles for individual use.